



## The emergence and growth of a submarine volcano: The Kameni islands, Santorini (Greece)



P. Nomikou<sup>a,\*</sup>, M.M. Parks<sup>b,c</sup>, D. Papanikolaou<sup>a</sup>, D.M. Pyle<sup>b</sup>, T.A. Mather<sup>b</sup>, S. Carey<sup>d</sup>, A.B. Watts<sup>b</sup>, M. Paulatto<sup>b</sup>, M.L. Kalnins<sup>b</sup>, I. Livanos<sup>a</sup>, K. Bejelou<sup>a</sup>, E. Simou<sup>a</sup>, I. Perros<sup>e</sup>

<sup>a</sup>University of Athens, Faculty of Geology and Geoenvironment, Panepistimioupoli Zografou, 15784 Athens, Greece

<sup>b</sup>Department of Earth Sciences, University of Oxford, South Parks Road, Oxford OX1 3AN, UK

<sup>c</sup>Nordic Volcanological Center, Institute of Earth Sciences, University of Iceland, Reykjavik IS-101, Iceland

<sup>d</sup>Graduate School of Oceanography, University of Rhode Island, Narragansett, USA

<sup>e</sup>University of Athens, Pedagogical Department of Primary Education, Greece

### ARTICLE INFO

#### Article history:

Available online 13 March 2014

### ABSTRACT

The morphology of a volcanic edifice reflects the integrated eruptive and evolutionary history of that system, and can be used to reconstruct the time-series of prior eruptions. We present a new high-resolution merged LiDAR-bathymetry grid, which has enabled detailed mapping of both onshore and offshore historic lava flows of the Kameni islands, emplaced in the centre of the Santorini caldera since at least AD 46. We identify three new submarine lava flows: two flows, of unknown age, lie to the east of Nea Kameni and a third submarine flow, located north of Nea Kameni appears to predate the 1925–1928 lava flows but was emplaced subsequent to the 1707–1711 lava flows. Yield strength estimates derived from the morphology of the 1570/1573 lobe suggest that submarine lava strengths are approximately two times greater than those derived from the onshore flows. To our knowledge this is the first documented yield strength estimate for submarine flows. This increase in strength is likely related to cooling and thickening of the dacite lava flows as they displace sea water. Improved lava volume estimates derived from the merged LiDAR-Bathymetry grid suggest typical lava extrusion rates of  $\sim 2\text{--}3\text{ m}^3\text{ s}^{-1}$  during four of the historic eruptions on Nea Kameni (1707–1711, 1866–1870, 1925–1928 and 1939–1941). They also reveal a linear relationship between the pre-eruption interval and the volume of extruded lava. These observations may be used to estimate the size of future dome-building eruptions at Santorini volcano, based on the time interval since the last significant eruption.

© 2014 The Authors. Published by Elsevier Ltd. Open access under [CC BY license](https://creativecommons.org/licenses/by/4.0/).

### Introduction

Analysis of lava flow morphology can improve our understanding of historical effusive eruptions by providing insights into the evolution of flow fields, lava effusion rates and bulk rheological properties (e.g., [31,14,5]). Lava flows are considered non-Newtonian and are often modeled as Bingham fluids, which require a critical shear stress (yield strength) to be exceeded to initiate viscous flow [34,19]. Determination of rheological properties (e.g., yield strength) provides insight into eruptive behaviour and the origin of flow morphologies (e.g., [12,38,21,30,3]). Morphological studies on terrestrial volcanoes reveal strong positive correlations between, for example, silica content and lava lobe width, which enables the estimation of lava flow compositions on Earth, and elsewhere, by remote sensing (e.g., [41]).

Prior work on the volcanology of Santorini has focused almost exclusively on observations of sub-aerial exposures of lava flows. No previous studies have attempted to understand the submarine volcanic activity that has accompanied the growth of the Kameni islands over the past few thousand years. Earlier work on the Kameni islands used a high resolution LiDAR dataset to map the subaerial extent of the historical dacite lava flows [31]. Pyle and Elliott [31] used a LiDAR dataset acquired in 2004 which comprised 4.52 million point measurements acquired over an area of  $\sim 8\text{ km}^2$ . Unfortunately a section of data was missing from the central part of Nea Kameni, due to absorption from low lying cloud. In addition, Pyle and Elliott [31] derived bulk rheological properties of these lava flows, and used the time-predictable nature of historic eruptions on Nea Kameni to develop a forecast for the duration of future dome-forming eruptions, based on the relationship between eruption length and the time interval between consecutive eruptions (pre-eruption interval).

\* Corresponding author. Tel.: +30 2107274865.

E-mail address: [evinom@geol.uoa.gr](mailto:evinom@geol.uoa.gr) (P. Nomikou).

This current study is based on a repeat LiDAR survey in May 2012, shortly after a period of volcanic unrest from January 2011 to April 2012, characterized by caldera-wide inflation and increased seismicity [25,29,8]. During this time, weather conditions were more favorable and full LiDAR coverage was achieved. In this paper, we also combine the new 2012 onshore LiDAR dataset with high-resolution swath bathymetry data, to determine for the first time, the morphology of the entire subaerial and submarine volcanic structure of the Kameni islands. This merged dataset provides complete coverage of the historic lava flows, enabling us to map the extent of both onshore and offshore extrusion events in the vicinity of the islands since AD 46 (Table 1 Of Supplementary Material). Updated lava flow outlines and thicknesses are used to refine estimates of erupted volumes for each of the historic flows, including previously unidentified submarine flows and cones. This allows a new analysis regarding the relationship between eruption volume and pre-eruption interval that may be used to forecast the size of future dome-forming events at Santorini.

## Methodology

The digital elevation model (DEM) of Santorini and the surrounding seabed was generated by merging onshore LiDAR data of the Kameni islands, high-resolution swath bathymetry of the seabed and a digitized elevation model of the Santorini island group from the Hellenic Military Geographical Service (HMGS).

Onshore LiDAR data was acquired over the central volcanic islands of Nea Kameni and Palea Kameni on the 16th May 2012 by the UK's Airborne Research and Survey Facility's (ARSF) Dornier 228 aircraft. The aircraft was equipped with a Leica ALS50 Airborne Laser Scanner, AISA Eagle and Hawk hyperspectral instruments, a Daedalus 1268 Airborne Thematic Mapper (ATM) and a Leica RCD105 39 megapixel digital camera. Two stand-alone georeferencing systems recorded position measurements at both the sensor and the aircraft frame [23]. The data were combined with ground control measurements from two local continuous GPS stations (MKMN and DSLN) to obtain accurate aircraft position measurements.

The survey comprised 12 north–south flightlines acquired in Single Pulse in the Air (SPiA) mode, at an altitude of  $\sim 1100$  m and average speed of 135 knots ( $70 \text{ ms}^{-1}$ ). An additional SW–NE flightline was acquired at an altitude of  $\sim 2000$  m and speed of 143 knots ( $74 \text{ ms}^{-1}$ ), using high resolution Multiple Pulse in the Air (MPiA) (e.g., [35]) LiDAR. The SPiA LiDAR was acquired using a pulse repetition frequency (PRF) of 94.7 kHz and scan frequency of 58.2 Hz. The MPiA flightline was acquired using a PRF of 119 kHz and scan frequency of 55.7 Hz. The final dataset comprised  $> 40$  million point measurements and provided an average point density of  $\sim 5$  points per  $\text{m}^2$ .

Following the application of a point cloud filter to remove noisy data points, we generated a new digital elevation model (DEM) from the 2012 LiDAR dataset using gridding functionality available in Generic Mapping Tools (GMT) software. To minimize the roll-oversight error (e.g., [40,11]) and the potential for acquisition artefacts in overlapping regions between adjacent flightlines, the point cloud data was resampled and filtered prior to gridding. The data points were then interpolated to a 2-m grid using a continuous curvature surface gridding algorithm.

Multibeam bathymetric surveys were carried out by R/V AEG-AEO of the Hellenic Centre for Marine Research (HCMR), during three cruises carried out in 2001 and 2006, covering an area of  $2.480 \text{ km}^2$  over the Santorini volcanic field [26]. The surveys utilized a 20 kHz, hull-mounted SEABEAM 2120 swath system, suitable for operation in water depths between 20 and 6000 m and at speeds up to 11 knots. The system forms 149 beams over a

maximum angular coverage of  $150^\circ$ , covering a swath width up to 7.5 times the water depth. The typical water depth in the survey area is 500 m, corresponding to a swath width of 3.75 km. The average position of the ship was determined to within  $\pm 10$  m by GPS navigation (Trimble 4000). The multibeam data processing included georeferencing using navigation data, removal of erroneous beams, noise filtering, interpolation of missing data and removal of rogue points (e.g., [2]).

The digital elevation model (DEM) of the Santorini outer island group (comprising the islands of Thera, Thirasia and Aspronisi) was produced by digitisation of height contours (interval 4 m) of the topographic maps of HMGS and by the triangulation network of HMGS with an accuracy of 4 cm. The three datasets were gridded together at 15 m interval using a continuous curvature polynomial method (Fig. 1). Due to the lack of shallow bathymetric measurements, interpolation was required for near-shore regions with water depths between 0 to 100 m (this corresponds to a maximum distance of  $\sim 330$  m offshore from the Kameni islands).

A higher resolution 5 m grid was obtained for the inside of Santorini caldera, providing a detailed onshore-offshore grid (Fig. 2) and enabling the first joint mapping of both subaerial and submarine historic lava flows emplaced since at least AD 46 in the centre of the Santorini caldera (Fig. 3 and Supplementary Figs. 1 and 2).

High-resolution merged LiDAR-Bathymetry grids have been utilised at other volcanoes for improved geomorphological analysis of volcanic deposits and to facilitate hazard mapping [17,32]. In the current study, a series of attribute maps were used to aid the delineation of the extent of flows (both onshore and offshore). These included hillshade, curvature and slope attributes generated using GMT software. The revised lava flow outlines were then used to compute accurate volumetric estimates for each of the historic flows.

Lava flow volumes were estimated in two ways. Firstly, volume calculations were carried out using Surfer software to determine the residual volume between two grid files, representing the post-eruption and the pre-eruption surfaces. This was done sequentially in the reverse chronological order to which the flows were originally emplaced. For example the first post-eruption surface is defined by the present-day grid of the Kameni islands. The first pre-eruption surface is the estimated topography prior to the most recent eruption in 1950. This was generated by stripping off the region within the outline of the 1950 lava flow and creating a new surface by interpolating the data gap using a Natural Neighbour Gridding Method. This method produces a smooth surface, simulating the relief prior to emplacement of the lava flow and was repeated for each of the historic flows so that the simulated pre-eruption grid becomes the post-eruption grid for the earlier lava flow. The volumes for the individual flows were generated by subtracting the hypothetical pre-eruption surfaces from the post-eruption surfaces. A similar DEM differencing technique was employed by Coltelli et al. [4] and Neri et al. [24] to determine lava flow volumes for historic eruptions at Mt Etna.

To gain a better understanding of the errors associated with the volume estimates, a second method was employed using GMT software. In this instance polygons outlining the flows from each historic eruption were again used to mask out the target flow from the DEM. This time the gap in the data was interpolated using the same continuous curvature surface gridding algorithm as was used to produce the present-day DEM, with the variable tension adjusted to derive a smooth near-flat pre-eruption surface across the masked region. In general we found that a tension of 0.9 was optimal to produce geologically reasonable surfaces with the exception of the 1950 flow, where a tension of 0.2 was used. The DEM subtraction technique was then used to compute the residual volume between the new pre- and

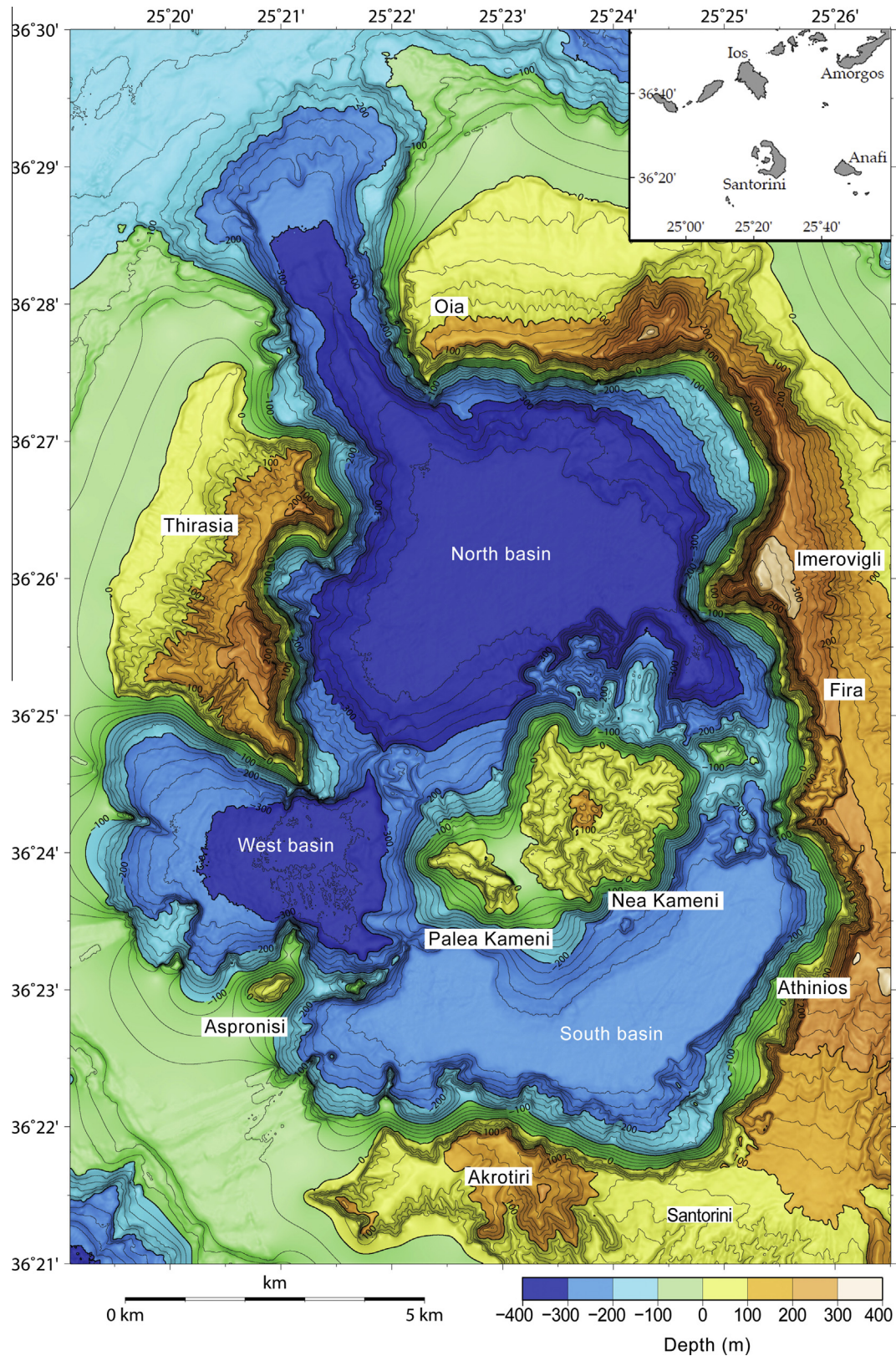


**Fig. 1.** Combined bathymetric and topographic map of Santorini Caldera with 15-m grid resolution. The study area encompassing the Kameni islands is located in the centre of the Santorini caldera.

post-eruption surfaces, providing a second set of volumetric estimates for each of the historic lava flows ([Supplementary Fig. 3](#) and [Supplementary Material](#)).

Pre-eruption interval was plotted against volume of extruded lava and eruption duration to determine the relationship between these eruptive properties. Finally a series of profiles were extracted

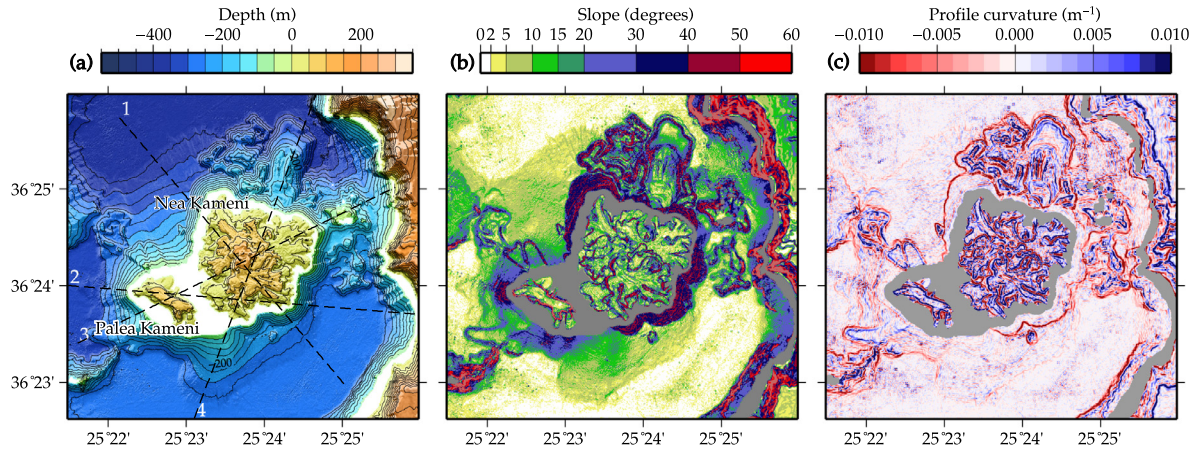


**Fig. 2.** Attribute maps of the Kameni islands: (a) detailed topographic map (onshore & offshore data), (b) slope distribution map, (c) profile curvature map. The white and grey areas indicate no swath data. Black dashed lines mark the cross-sections shown in Fig. 4.

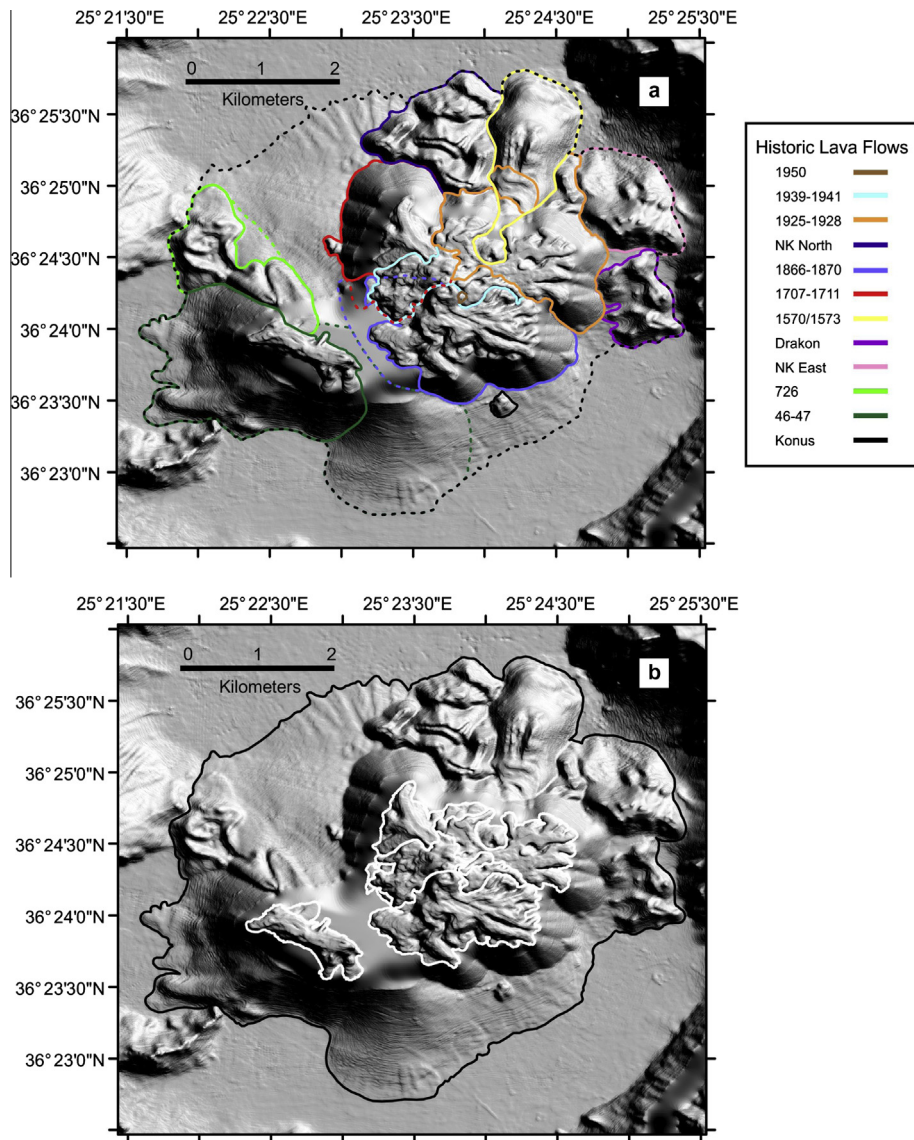


**Fig. 3.** Lava flow outlines for historic lava flows in the vicinity of the Kameni islands. (a) New onshore/offshore lava flow outlines, mapped as part of this study. For the 46–47, 726, 1707–1711 and 1866–1870 flows the solid lines represent the minimum extent of the flows and the dashed line the possible maximum extent. The maximum extent of submarine talus deposits is shown by the black dashed line. (b) Onshore lava flows mapped by Pyle and Elliott [31] (white contours). The black contour represents the maximum extent of submarine talus deposits mapped during the current study.

from the DEM to determine flow height and flow width for the off-shore segment of the 1570/1573 lava flow and estimates of yield strength were derived, assuming a Bingham rheology and using the flow width method [12,13].

## Results and discussion

The new DEM of Santorini Caldera (Fig. 1) is the foremost high-resolution merged dataset since Druitt et al. [6], who initially presented a relief model of Santorini caldera showing the subaerial topography and submarine bathymetry. The caldera walls rise to over 300 m above sea level, while the maximum depth of the caldera seafloor is about 390 m below sea level. The present configuration of the caldera consists of three distinct basins that form separate depositional environments [28]. The North Basin is the largest and the deepest (389 m) developed between the Kameni islands, Thirasia and the northern part of the Santorini caldera. It is connected by a narrow steep-sided channel with a depth of 300 m to a scallop-shaped ENE–WSW aligned feature that lies outside Santorini caldera, NW of Oia Village.

The smaller West Basin is encompassed by Aspronisi islet, Palea Kameni and Southern Thirasia with a moderate maximum depth – up to 325 m. The flanks of the basin are gentle in the western part and steeper close to Thirasia and Aspronisi. The South Basin is bounded by the Kameni islands (to the north) and the southern part of the Santorini caldera (to the south). It covers a larger area and is shallower by ~28 m than the western basin. The seafloor morphology suggests that the southern basin has been separated from the western and northern basins by the development of a series of subaerial and submarine volcanic domes, aligned in a NE–SW direction. Apart from the subaerial Kameni islands, the most well-known submarine extrusion is the reef close to Fira Port (referred to here as NK East), which has grown from 300 up to 40 m b.s.l.

The Kameni islands reach a total relief of almost 470 m in the central part of the Caldera and cover an area of ~21 km<sup>2</sup>, assuming a perimeter represented by the black dashed line around Kamenis on Fig. 3. The submarine structure of the islands to the north and to the south is very different. Submarine lava flows can be observed to the east (NK East and Drakon), NE and NW of Nea Kameni and WSW of Palea Kameni (Fig. 3). In contrast, the southern part of Nea Kameni is characterised by abrupt submarine volcanic cliffs up to 250 m high [26,28].

### Mapping of historic lava flows

The new high-resolution DEM of the Kameni Islands and the surrounding seabed reveals intricate details of the surface morphology (from 380 m b.s.l. up to 127 m a.s.l) of young dacite lava flows, cones and domes (Fig. 2a), from which important morphological information can be extracted. The lava flows identified in the LiDAR data can now be followed beyond the shoreline and onto the sea floor, specifically the submarine continuation of historical lava flows in the northern part of Nea Kameni and at the NW and SW part of Palea Kameni. The ridge east of Aspronisi connecting to the Kameni islands edifice (Fig. 1) may be made up of young lava domes as suggested by Sigurdsson et al. [36], or it may represent a ridge of older rocks (continuation of the Aspronisi islet) isolated by collapse events from the western and southern basins. The submarine structures, east of Aspronisi are highlighted in the slope steepness plot, as are the volcanic domes east of Nea Kameni (Fig. 2b). There is also an individual small volcanic dome-like structure south of Nea Kameni named Konus (Fig. 3a) which could also represent a large block that has fallen off Nea Kameni.

Pyle and Elliott [31] suggested that the Kameni line (a proposed active volcano-tectonic fault/fracture zone) may control vent locations for both historic and future dome building eruptions on the Kameni islands. Our dataset corroborates this hypothesis; as the submarine volcanic dome within the NK East flow (40 m depth) [27] and the potential submarine volcanic domes east of Aspronisi [36,28] continue the NE–SW trend following the Kameni Line as defined by the volcanic vents across the Kameni Islands [10,6,7,31]. Furthermore, the Kameni Line appears to divide the flooded caldera.

The attribute maps (displayed in Fig. 2b, c) assisted in mapping the extent of the submarine and subaerial historic lava flows extruded in the centre of the caldera since 46AD. Fig. 2b shows the distribution of slope gradient within the studied area and allows the identification of five zones: (1) sub-horizontal areas with mean morphological slope 0–5°, (2) low-slope areas of 5–15°, (3) moderate-slope areas of 15–30°, (4) high-slope areas of 30–40° and (5) very steep slope areas of >40°. The distribution of the slope magnitudes illustrates the homogeneous areas of smooth or uneven relief as well as the zones along which there is an abrupt change of slope. Areas of abrupt slope change correspond either to the rim and base of the inner wall of Santorini Caldera or to the edges of lava flows on the submarine slopes of Nea Kameni. The steep terrestrial slopes of the Caldera continue with the same magnitude below sea level, showing the same vertical precipitous character from >40° until the level of the caldera floor (0–5°). The submarine structures east of Aspronisi island have a linear distribution NE–SW (Fig. 1) and show an abrupt change of slope from >40° to (0–5)°. The summits of these structures are flat and their external flanks are very steep forming the physical barrier between the West and South basin. On the other hand the volcanic dome approximately mid-way between Nea Kameni and Fira port, has steep external slopes, up to 40°, with a wider flat crater-like structure at the top. Moderate-slope areas characterize the slopes of the smaller submarine volcanic domes south of NK East, some of which reveal suggestions of crater-like structures at their summit.

The volcanic edifices of the Kameni islands continue below sea level with a perimeter zone of abrupt slopes (20–40° and >40°) which diminishes sharply to 0–5° and is interrupted only by lava flows at the northern part of Nea Kameni and NW and SE of Palea Kameni. Submarine lava flows have high frontal slope values (20–40°) but moderate slopes (10–20°) on the rest of the lava surface. Similarly the on-shore lava flows from various historic eruptions on Nea Kameni display relatively steep slopes combined with extended relatively low slope surfaces on the body of the flows. This morphology is indicative of the relatively young age of the volcanic activity of the islands [31].

Palea Kameni has steep on-shore slopes in the SE part with an axial structure trending NW–SE, and a planar surface at the top up to >100 m in height. The submarine slope gradient around the island diminish gradually from 20–40° to 5–10° with the exception of lava flows to the SW and NW of the island. These submarine lava flows are characterized by moderately sloping tops dipping at 10–20° with steep frontal slopes of 20–40°.

The profile curvature map of Nea Kameni (Fig. 2c) is calculated by computing the second horizontal derivative of the DEM surface in the direction of the maximum slope. Areas of high positive curvature represent upwardly concave regions (hills) whereas negative curvatures depict upwardly convex regions (valleys). This attribute was useful in delineating the edges of different historic lava flows. It also highlights some channel levées and compression folds, both in the onshore and offshore data. Levée structures, tens of meters wide and tens of meters high, develop close to the vents. Channelized flows within the levées show prominent ridges with wavelengths ~20–40 m and amplitudes ~1–4 m at the northeastern offshore part of Nea Kameni.

Fig. 3 shows the new onshore/offshore lava flow outlines which were used to calculate revised volumetric estimates for each of the historic flows and generate graphs of pre-eruption interval against the volume of extruded lava (section ‘Volume estimates and rates of lava effusion’). Given the challenges of correlating lava flows from onshore and offshore locations, and attributing lobes covered over by subsequent flows, there are considerable uncertainties in these estimates. The lack of data between depths of 0–100 m adds to these uncertainties. While we made reasonable correlations given the data in hand, some of these correlations remain uncertain, and there may well be older flows which have not been identified. For example, the eruption of 197 B.C. apparently produced a large island called Hiera (see [9,31]), which must have later subsided. Fouqué [9] suggested this corresponded to a submarine reef, called Bancos, that lay between Nea Kameni and Fira. Bancos was subsequently buried by the 1925–1928 lavas. Likewise, there are assumptions inherent in the onshore-offshore correlations made for the 46–7, 726 and 1570/73 flows. The records of these eruptions are scant but, for example, Fouqué [9] reports that 17th Century accounts of the 1570/1573 eruption suggest that it lasted for a year, so it is not unreasonable that it might have formed as substantial a lava flow as we infer. These three flows are not included in the graphs of pre-eruption interval against the volume of extruded lava (section ‘Volume estimates and rates of lava effusion’). We attempt to take account of these uncertainties by constructing minimum and maximum polygons for several of the flows (46–47, 726, 1707–1711 and 1866–1870). For the 46–47, 726, 1707–1711 and 1866–1870 flows the solid line in Fig. 3a represents the possible minimum extent and the dashed line the possible maximum extent. These multiple flow outlines were used in the volumetric calculations to provide a range of estimates.

Cross-sectional profiles are shown in Fig. 4, traversing both onshore and offshore lava flows (Fig. 2a). The first profile (NW–SE)

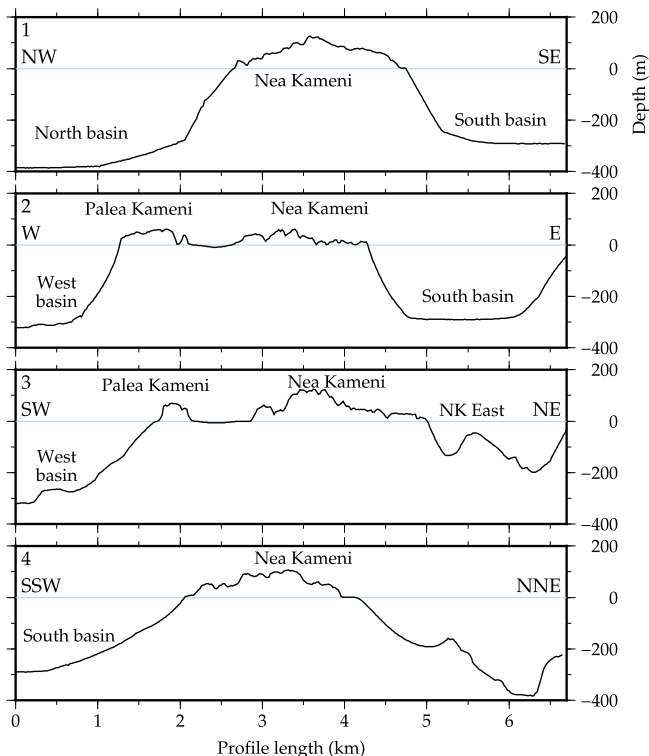


Fig. 4. Elevation profiles across the Kameni islands: profile 1 across Nea Kameni orientated in NW–SE direction, profile 2 across Nea Kameni orientated W–E direction, profile 3 across Palea and Nea Kameni orientated in SW–NE direction, profile 4 across Nea Kameni orientated in SSW–NNE direction.

starts east of Thirasia island and terminates close to Athinios port, in the southern part of the caldera. It cuts the flat part of the North Basin at the depth of 380 m b.s.l. and shows the gently dipping talus and the steep submarine slopes of Nea Kameni, terminating in the flat part of the South Basin (280 m b.s.l.). In this profile, the depth difference between the two submarine basins, separated by Nea Kameni is clearly shown. The second profile (WNW–ESE) starts at the depth of 320 m b.s.l., displaying the flat bottom of the Western Basin interrupted by the abrupt slopes of lava flows from Palea Kameni. The flat top of the oldest lava of Palea Kameni and the rough volcanic relief of Nea Kameni island are also distinguishable. The profile crosses the flat bottom of the Southern Basin which is shallower than the Western Basin and ends on the slope of the caldera wall. It is clear that both islands constitute the majority of the overall volcanic relief between the two basins.

The third profile (SW–NE) starts in the southern part of the Western basin around 320 m depth and terminates at Fira Port. Starting in the west, one can observe the abrupt southwestern submarine slopes of Palea Kameni, the onshore Palea Kameni AD 46–47 lava flows, the topography of Nea Kameni; including the area of the central vents and the surface of the 1925–1928 lava flows at the northeastern part of the island and the submarine channel between Nea Kameni and the NK East submarine volcanic dome. This profile highlights that the NK East dome, also characterized by steep slopes and a top at 40 m depth, belongs to the same volcanic structure as Nea and Palea Kameni. The last profile (SSW–NNE), starts from the flat bottom of the South Basin and ends on the abrupt submarine slopes of Skaros point. It cuts along the submarine 1570/1573 lava lobe, revealing that the smooth surface of the flow observed onshore continues to a depth of 200 m. The volcanic morphology of Nea Kameni is also shown in this profile, which bisects different lava levées, as well as the highest central part of the island (containing the majority of the craters). The southern submarine slopes of Nea Kameni are more gentle without any recent lava extrusions. It is worth noting that the total volcanic edifice of Palea and Nea Kameni rises from 380 m b.s.l. in the north, 290 m b.s.l. in the south, 320 m b.s.l. in the west and 200 m b.s.l. in the east, outlining the limits of the total volcanic edifice (see black dotted line in Fig. 3a).

#### Flow identification, morphologies and yield strength

The new dataset provides a wealth of information, including previously unidentified submarine lava flows and cones, as well as some interesting submarine morphologies. Lava flow morphologies are dependent on a number of factors, including the temperature, yield strength, viscosity, effusion rate and local topographic gradient [16], and references therein). Although several morphological studies have been undertaken on the subaerial-submarine transition of lava flows these have been mostly limited to basaltic pāhoehoe and ‘a’ā flows (e.g., [20,39,37]). The historic flows emplaced on Nea Kameni since 1570/1573 are classified as blocky lava flows. These flows are characterized by a broken fractured crust, comprising smooth angular blocks of dm- to m-scale. The flows are typically tens of meters thick and several kilometers long. Blocky lava flows tend to advance as single units, forming channels and occasional lava tubes [15]. These in turn feed the advancing lava front, which crumbles to produce a snout and may trigger small block and ash flows. Overflow levees develop along the edges of channels as the crust along the channel margin begins to cool and solidify. An example of this may be seen in the medial section of the 1570/1573 submarine flow and also in a flow situated offshore, north of Nea Kameni (NK North) (Fig. 3). An archetypal example of a single feeder channel is visible in the centre of the 1707–1711 lava flow, on the north–west edge of Nea Kameni (indicated by a black arrow in Fig. 5). Flow breaching is less common in

blocky lava flows. However, a good example is visible within the onshore 1707–1711 lava flow and possibly within a thin channel in the central portion of the NK north flow (Fig. 3).

Although there are typically more similarities between onshore pāhoehoe and blocky lava flows in terms of the crust and flow emplacement mechanisms, our dataset suggests that during and following the subaerial-submarine transition dacitic blocky lava flows may in fact have more in common with ‘a‘ā flows. Both Stevenson et al. [39] and Mitchell et al. [20] observed that during the subaerial-submarine transition of pāhoehoe and ‘a‘ā flows, the pāhoehoe flows exhibited a significant change in slope upon entering the water and were more likely to become arrested, whereas the ‘a‘ā flows remained comparatively unchanged and often advanced for several hundred meters. Several similarities are apparent between the documented transitional behavior of ‘a‘ā flows and the Nea Kameni 1570/1573 lava flows. The feature that we interpret as the submarine lava lobe from the 1570/1573 eruption displays a well-rounded margin likely developed via lateral spreading of the lava front [15], and continues to extend offshore for several hundred meters. If our interpretation of this flow is correct, then it would appear that the marine transition had little impact on the reduction of flow length for blocky dacitic flows – most likely attributable to the substantial flow thickness which in turn minimizes internal cooling.

Thin channels and possible tumulus-like structures are identified to the north of Nea Kameni within the NK north flows (Fig. 3a). The latter were identified during a cruise undertaken in 2011 on board E/V Nautilus. They are possibly formed by the influx of new lava increasing the internal pressure and fracturing of the outer crust. Other evidence for flow pressurization may include the longitudinal cleft identified in the center of the 1570/1573 off-

shore lava lobe. This likely developed from the extension of a solidified, chilled crust via the continued movement and pressurization of a fluid core (e.g., [20]) or via lateral spreading on a convex upwards surface.

Figs. 5 and 6 display a series of elevation profiles across each of the historic lava flows. Of particular interest are the submarine extension of the 1570/1573 flow, the NK East and Drakon flows to the east of Nea Kameni and a newly identified submarine flow NK North. The new flow was initially interpreted as an extension of the onshore 1925–1928 lavas because of its proximal location. However, following the analysis of elevation, slope and hillshade attributes (Fig. 2) along with volume calculations and historic reports [31], we suggest that these flows were extruded during an unreported submarine eruption. Analysis of flow morphologies suggests this extrusion occurred sometime after the 1707–1711 eruptions, but prior to the 1925–1928 eruption. The internal structure of the NK North flow suggests that the flow paths were determined by the pre-existing topography of the 1707–1711 flow and an obvious break in slope is visible on both the hillshade attribute and the north–south oriented traverses that transect both the NK North and 1925–1928 flows (Fig. 6(a) and (e)). This break in slope appears at the edge of submarine talus deposits eroded off the 1925–1928 flows, which were identified during an oceanographic cruise in September 2011 [27]. In addition, the general morphology of the flow also changes significantly after this break in slope and is more similar to that observed on the Drakon lava flows, exhibiting submarine twin cone structures and intervening ridges. This morphology appears to be characteristic of submarine extrusions/eruptions; and has been identified on El Hierro, Canary Islands [33] and in the Marianas Arc [1].

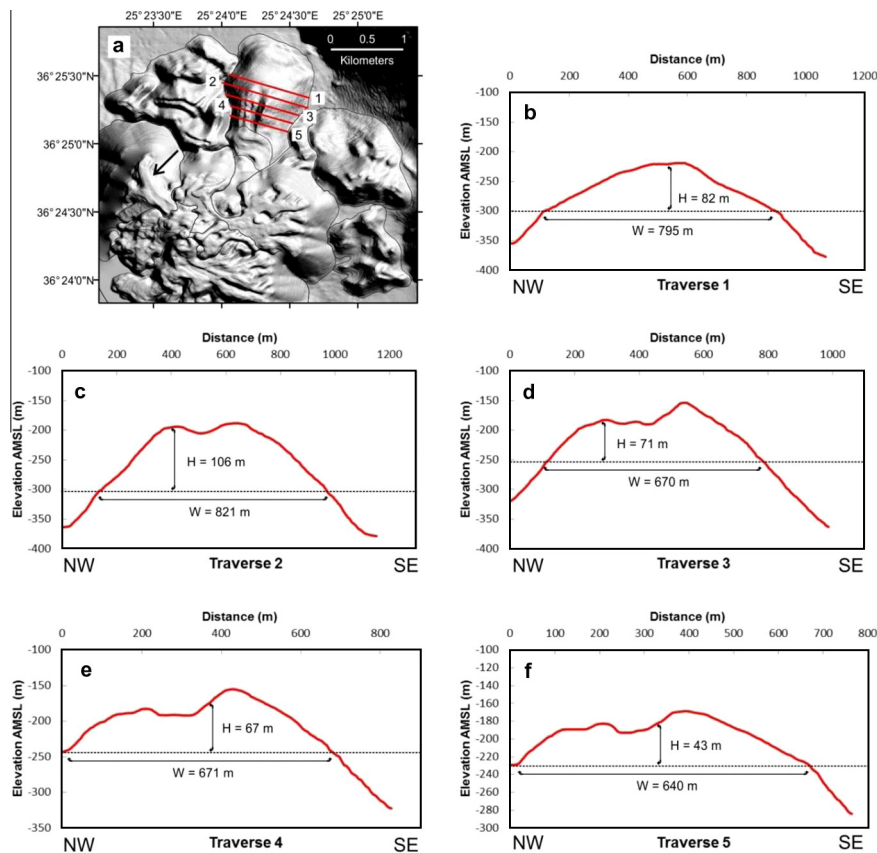


**Fig. 5.** Elevation profiles across the submarine 1570/1573 lava lobe. (a) 5 m resolution merged onshore/offshore digital elevation model. The arrow displays the location of the 1707–1711 feeder channel referred to in text. (b–f) Traverses across the historic submarine 1570/1573 lava lobe showing heights and widths used to estimate the yield strength of the lava.

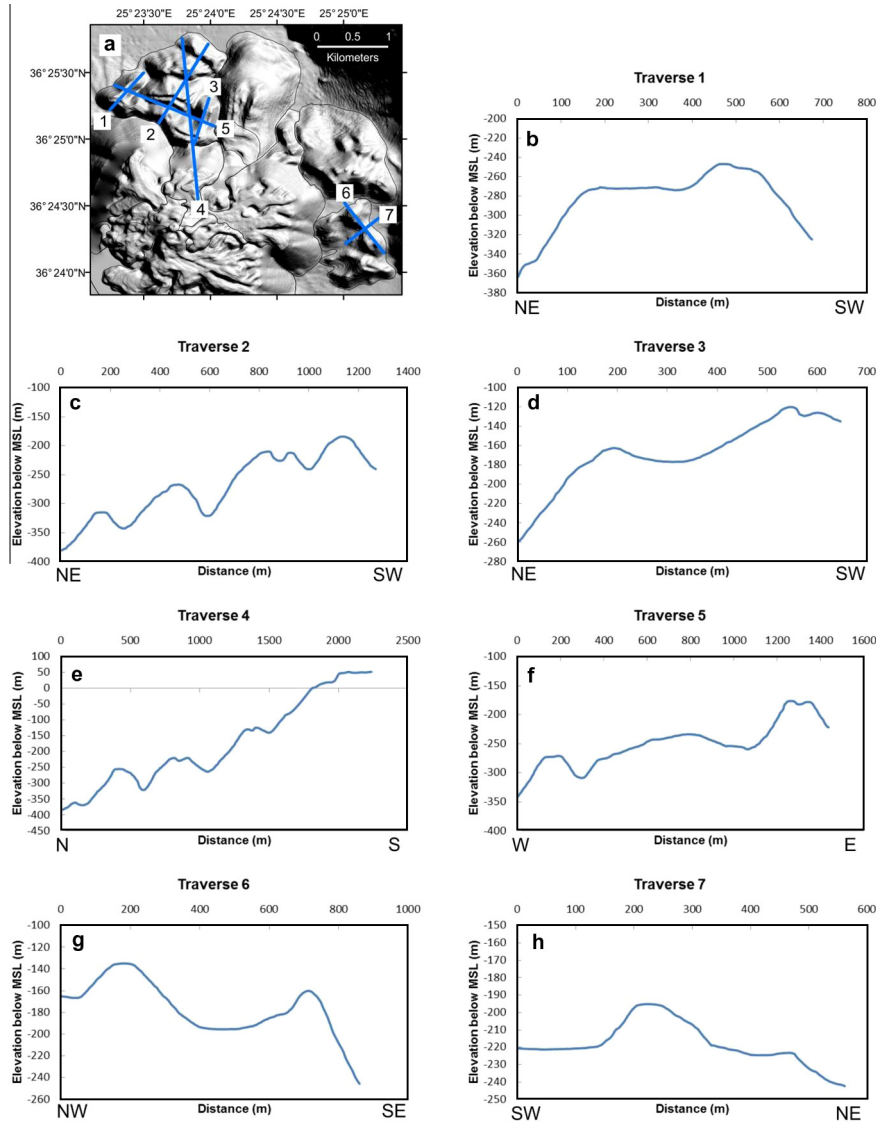


**Fig. 6.** Elevation profiles across the NK North, 1707–1711 and Drakon lava flows. (a) 5 m resolution merged onshore/offshore digital elevation model. (b–f) Traverses across the NK North (north of Nea Kameni) and 1707–1711 lava flows. (g,h) Traverses across the Drakon (east of Nea Kameni) submarine lava flow.

To enable comparison of yield strength estimates for onshore lava flows (computed by [31] with those of offshore lava flows, yield strengths were calculated for the submarine 1570/1573 lava lobe using flow widths and heights extracted from a series of transverse profiles displayed in Fig. 5. The 1570/1573 flow was determined to be the most suitable submarine flow for this calculation due to its characteristic lava lobe morphology discussed above. The flow width method [12,13] was used for this analysis, as it is considered more reliable than the levée width or levée height methods [38,31], based on the larger uncertainties associated with the latter techniques in estimating the flow slope (at the time of emplacement) and the levée width. For a lava flow

of width  $W$ , on a flat surface, the yield strength  $Y$ , may be calculated using equation 1:

$$Y = \frac{\Delta\rho gh^2}{W} \tag{1}$$

where  $\Delta\rho$  is the density contrast between the lava flow and seawater (taken as  $1680 \text{ kg m}^{-3}$ ),  $h$  is the height of the lava flow and  $g$  is the gravitational acceleration. The yield strength estimates are displayed in Table 1. The submarine lava flow displays an average width of 719 m, height of 74 m and yield strength of  $(129 \pm 64) \times 10^3 \text{ Pa}$ . This is approximately twice as large as estimates reported by Pyle and Elliott ([31] Table 3) for onshore lava

**Table 1**  
Yield strength estimates for the 1570/1573 submarine dacite lava flow. Traverses refer to those shown in Fig. 5.

	Flow height (m)	Flow width (m)	Aspect ratio (flow height/flow width)	Yield strength ( $\times 10^3 \text{ Pa}$ ) (Flow width method)
Traverse 1	82	795	0.103	139
Traverse 2	106	821	0.129	226
Traverse 3	71	670	0.106	124
Traverse 4	67	671	0.100	110
Traverse 5	43	640	0.067	48
Average	74	719	0.101	129

**Table 2**  
Volume estimates of historic lava flows extruded in the vicinity of the Kameni islands since AD 46.

Eruption	Pre-eruption interval <sup>a</sup> (yr)	Eruption length (days)	GMT minimum volume (km <sup>3</sup> )	GMT maximum volume (km <sup>3</sup> )	Surfer minimum volume (km <sup>3</sup> )	Surfer maximum volume (km <sup>3</sup> )	Average Volume (km <sup>3</sup> )
Konus	–	–	0.00067	0.00067	0.00063	0.00063	0.00065
1950	9	23	0.000014	0.000014	0.000004	0.000004	0.000009
1939–1941	11	682	0.011	0.011	0.010	0.010	0.01054
1925–1928	55 <sup>b</sup>	949	0.092	0.092	0.072	0.072	0.082
NK	North	–	–	0.0525	0.0525	0.057	0.057
0.055							
1866–1870	155	1723	0.170	0.244	0.125	0.139	0.17
1707–1711	137	1575	0.094	0.15	0.081	0.113	0.11
1570	844	–	0.0665	0.068	0.069	0.069	0.068
Drakon	–	–	0.0160	0.0160	0.0169	0.0169	0.0164
NK East	–	–	0.048	0.048	0.041	0.041	0.044
726	679	–	0.019	0.022	0.017	0.023	0.020
46–47	–	–	0.134	0.178	0.100	0.143	0.139
		Total	0.70	0.88	0.59	0.69	0.72 <sup>c</sup>

<sup>a</sup> The pre-eruption interval is the time between consecutive eruptions.

<sup>b</sup> This represents the interval between 1870 and 1925. It is possible the NK North lava flow was extruded during this time period, however the date of this extrusion is currently unknown.

<sup>c</sup> The average volume is the average of all 4 max and min values using GMT and Surfer software.

**Table 3**  
Effusion rate estimates.

Eruption	Approximate flow duration (d)	Volume (km <sup>3</sup> )	Minimum effusion rate (m <sup>3</sup> s <sup>-1</sup> )	Maximum effusion rate (m <sup>3</sup> s <sup>-1</sup> )
1939–1941	147–282	0.01	0.4	0.8
1925–1928	230–263	0.08	3.5	4.0
1866–1870	690–1090	0.17	1.8	2.9
1707–1711	300–600	0.11	2.1	4.2
Average			1.9	3.1

Note: The anomalous 1950 eruption is interpreted as a minor extrusion of remnant magma, following the 1939–1941 activity [31], and has not been included in this calculation.

flows on Nea Kameni using the same technique, but still within the range of yield strength estimates derived from dacitic lava flows at other volcanoes (10<sup>4</sup>–10<sup>6</sup> Pa) [41]. To our knowledge this is the first documented yield strength estimate for submarine lava flows. The increase in apparent yield strength may reflect the transition from subaerial to submarine emplacement and is likely associated with increased cooling of the outer margins of the flow [12,18,22] or possibly a result of flow thickening during the onshore/offshore transition [37].

#### Volume estimates and rates of lava effusion

Table 2 summarises the revised lava flow volume estimates for each of the historic eruptions of the Kameni islands. This includes estimates for two separate offshore flows east of Nea Kameni (NK East and Drakon), one north of Nea Kameni (NK North) and a small

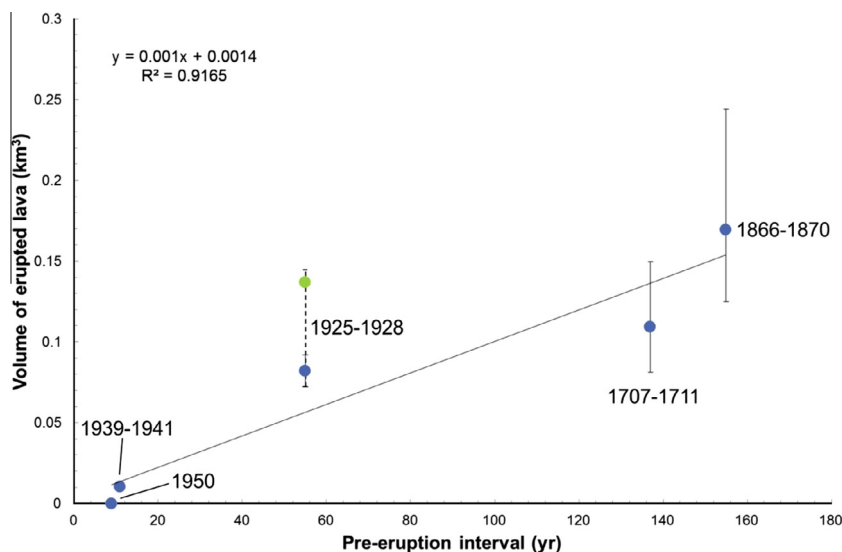


**Fig. 7.** Volume of erupted lava plotted against pre-eruption interval for the historic dome-forming eruptions on Nea Kameni. The green filled circle indicates the combined volume of the NK North and 1925–1928 lava flows (assuming both flows were extruded during 1925–1928). This data point was not incorporated in the linear regression. The associated blue point represents the volume of the 1925–1928 lava flow (as indicated in Fig. 3), which was incorporated in the linear regression. (For interpretation of the references to colour in this figure legend, the reader is referred to the web version of this article.)

cone identified offshore, south of the 1866–1870 flow (Konus). In Table 3, we estimate lava effusion rates for four historic eruptions (1939–1941, 1925–1928, 1866–1870 and 1707–1711) on Nea Kameni. This analysis suggests a typical effusion rate during dome-forming eruptions on Nea Kameni of  $\sim 2\text{--}3\text{ m}^3\text{ s}^{-1}$ . This is almost twice the average rate derived from the onshore data alone [31].

Fig. 7 reveals a linear relationship between pre-eruption interval (the intervening period between eruptions from historical records) and the volume of lava extruded in historic dome-forming eruptions. This correlation allows estimation of the size of future eruptions on Nea Kameni – for example, if an eruption were to occur in the next few years the pre-eruption interval period would be  $\sim 75$  years (time since the last significant eruption on Nea Kameni from 1939 to 1941). The volume of extruded lava would be of order  $8 \times 10^7\text{ m}^3$  and the eruption would continue for 2–3 years. Geodetic studies suggest that a possible melt volume of  $1\text{--}2 \times 10^7\text{ m}^3$  has already been supplied to the shallow magma chamber during the recent (2011–2012) period of unrest [25,29].

#### Long-term rates of lava effusion and edifice growth

The total volume of the Kameni islands is  $3.2\text{ km}^3$ , of which about  $0.5\text{ km}^3$  has erupted since 1570 AD (Table 2). Although it is clear that the entire Kameni edifice has formed and grown since the caldera-forming Minoan eruption of ca. 1600 BC, there are few constraints on when post-caldera volcanism began. The earliest reports, from Strabo, that are interpreted as evidence of an emergent island date back to 199–197 BC (Supplementary Table 1), though archaeologists have speculated that an earlier volcanic event may have triggered the departure of residents from Santorini and the formation of Cyrene in 630 BC [42]. Since 1570 AD, assuming that the most significant eruptions have been detected, the time-averaged extrusion rate (covering both periods of eruption and repose) has been  $\sim 10^6\text{ m}^3/\text{yr}$ , or  $0.035\text{ m}^3\text{ s}^{-1}$ . At these extrusion rates, the entire edifice of the Kameni islands would have been extruded in around 3200 years which is within the bounds of the time period since the Minoan eruption. If average lava extrusion rates have been approximately constant since the initiation of the extrusion of the Kameni Islands, this suggests that the first post-caldera eruptions started around 1200 B.C. long before the first historical reports of the islands emerging in 199 B.C.

#### Conclusions

This study highlights the benefits of combining high-resolution LiDAR and multibeam bathymetry data to accurately map the sub-aerial and submarine extensions of lava flows at partially submerged island volcanoes. The new dataset reveals a wealth of information regarding the emplacement of historic lava flows and insight into bulk rheological properties of the magma. Several previously undetected submarine flows have been identified off the northern and eastern coasts of Nea Kameni. The ages of the NK East and Drakon flows are currently unknown, however the NK North flow appears to have been emplaced prior to the 1925–1928 lava flows but subsequent to the 1707–1711 lava flows. Apparent yield strength estimates from the submarine 1570/1573 flow suggest a twofold increase in lava strength upon entering the ocean.

Accurate volumetric estimates derived from the merged LiDAR-Bathymetry grid suggest typical lava extrusion rate of  $\sim 2\text{ m}^3\text{ s}^{-1}$  during historic eruptions on Nea Kameni, which is approximately two times faster than the initial estimate by Pyle and Elliott [31] based solely on onshore data. The new volumetric estimates have allowed us to expand on the original work of Pyle and Elliott

[31], in terms of forecasting the characteristics of future eruptions at the Kameni Islands. We present a new relationship between the volume of erupted lava and the intervening period between eruptions based on the revised volumetric estimates. This will enable forecasting of the magnitude of new lava extrusions on the Kameni Islands at the onset of future dome-forming eruptions. Our volume estimates of flows emplaced since 1570 AD lead to an average extrusion rate of  $\sim 10^6\text{ m}^3/\text{yr}$ . At this rate the entire Kameni islands edifice could have been emplaced in  $\sim 3200$  years suggesting that activity here may have started around 1200 B.C., shortly after the Minoan eruption.

#### Acknowledgements

Multibeam data were obtained aboard R/V AEGAE0 of HCMR, during 2001 (in the framework of GEOWARN project, IST-1999-12310) and 2006 (THERA 2006, OCE-0452478, supported by a grant from the National Science Foundation). Matina Alexandri and Dionissis Ballas are gratefully acknowledged for their important and effective contribution during these cruises. We thank the captain and crew of the R/V AEGAE0 for their help and great skill in carrying out the exploration of Santorini volcano. Onshore data were collected during the Natural Environment Research Council (NERC) Airborne Remote Sensing Facility (ARSF) campaign to the eastern Mediterranean in May 2012. This work was supported by the National Environmental Research Council (NERC) through an urgency grant NE/J011436/1, and through the National Centre for Earth Observation (NCEO) of which COMET+ is a part. MP was supported through an NCEO studentship. TM acknowledges further support from the Leverhulme Trust.

#### Appendix A. Supplementary data

Supplementary data associated with this article can be found, in the online version, at <http://dx.doi.org/10.1016/j.grj.2014.02.002>.

#### References

- [1] Bloomer SH, Stern RJ, Smoot NC. Physical volcanology of the submarine Mariana and Volcano Arcs. *Bull Volcanol* 1989;51(3):210–24.
- [2] Cares DW, Thomas H, Kirkwood WJ, McEwen R, Henthorn R, Clague DA, Paull CK, Paduan J, Maier KL. High-resolution multibeam, sidescan, and subbottom surveys using the MBARI AUV D. Allan B. Mar Habitat Mapp Technol Alaska 2008:47–69.
- [3] Cigolini C, Borgia A, Cassertano L. Intracrateric activity, aa-block lava, viscosity and flow dynamics: Arenal Volcano, Costa Rica. *J Volcanol Geoth Res* 1983;20:155–76.
- [4] Coltellì M, Proietti C, Branca S, Marsella M, Andronico D, Lodato L. Analysis of the 2001 lava flow eruption of Mt. Etna from three-dimensional mapping. *J Geophys Res* 2007;112(F2):112.
- [5] Deardorff ND, Cashman KV. Emplacement conditions of the c. 1,600-year bp Collier Cone lava flow, Oregon: a LiDAR investigation. *Bull Volcanol* 2012;74(9):2051–66.
- [6] Druitt TH, Mellors RA, Pyle DM, Sparks RSJ. Explosive volcanism on Santorini, Greece. *Geol Mag* 1989;126(2):95–126.
- [7] Druitt TH, Edwards L, Mellors RM, Pyle DM, Sparks RSJ, Lanphere M, Davies M, Barreiro B. Santorini volcano. *Geol Soc London Mem* 1999;19:129–32.
- [8] Foulmelis M, Trasatti E, Papageorgiou E, Stramondo S, Parcharidis I. Monitoring Santorini volcano (Greece) breathing from space. *Geophys J Int* 2013;193(1):161–70.
- [9] Fouqué F. Translated and annotated by. In: McBirney AR, editor. *Santorini and its eruptions*. Baltimore: The Johns Hopkins Press; 1999.
- [10] Fytikas M, Kolios N, Vougioukalakis G. Post-Minoan activity of the Santorini volcano: volcanic hazard and risk, forecasting possibilities. In: Hardy DA, Keller J, Galanopoulos VP, Flemming NC, Druitt TH, editors. *Thera and the Aegean World III*, vol. 2. 1990. p. 183–98.
- [11] Glennie C. Rigorous 3D error analysis of kinematic scanning LiDAR systems. *J Appl Geodesy* 2007;1(3):147.
- [12] Hulme G. The interpretation of lava flow morphology. *Geophys J Int* 1974;39(2):361–83.
- [13] Hulme G, Fielder G. Effusion rates and rheology of lunar lavas. *Philos Trans R Soc London Ser A* 1977;285(1327):227–34.

- [14] James MR, Varley N. Identification of structural controls in an active lava dome with high resolution DEMs: Volcán de Colima, Mexico. *Geophys Res Lett* 2012;39(22).
- [15] Kilburn CR, Lopes R. General patterns of flow field growth: aa and blocky lavas. *J Geophys Res* 1991;96(B12):19721–32.
- [16] Maeno F, Taniguchi H. Silicic lava dome growth in the 1934–1935 Showa Iwojima eruption, Kikai caldera, south of Kyushu, Japan. *Bull Volcanol* 2006;68(7–8):673–88.
- [17] Massimo F, Baldi P, Anzidei M, Pesci F, Bortoluzzi G, Aliani S. High resolution topographic model of Panarea Island by fusion of photogrammetric, lidar and bathymetric digital terrain models. *Photogram Rec* 2010;25(132):382–401.
- [18] Marsh BD. On the crystallinity, probability of occurrence, and rheology of lava and magma. *Contrib Miner Petrol* 1981;78(1):85–98.
- [19] McBirney AR, Murase T. Rheological properties of magmas. *Annu Rev Earth Planet Sci* 1984;12:337–57.
- [20] Mitchell NC, Beier C, Rosin PL, Quartau R, Tempera F. Lava penetrating water: submarine lava flows around the coasts of Pico Island, Azores. *Geochem Geophys Geosyst* 2008;9(3):Q03024.
- [21] Moore HJ, Arthur DWG, Schaber GG. Yield strengths of flows on the Earth, Mars, and Moon. In: *Lunar and planetary science conference proceedings*, vol. 9. 1978. p. 3351–78.
- [22] Murase T, McBirney AR, Melson WG. Viscosity of the dome of Mount St. Helens. *J Volcanol Geoth Res* 1985;24(1):193–204.
- [23] NERC. Navigation systems aboard D-CALM. Available: <<http://arsf.nerc.ac.uk/instruments/navigation.asp>>; 2011 [Last accessed 7.02.14].
- [24] Neri M, Mazzarini F, Tarquini S, Bisson M, Isola I, Behncke B, Pareschi MT. The changing face of Mount Etna's summit area documented with Lidar technology. *Geophys Res Lett* 2008;35(9):L09305.
- [25] Newman AV, Stiros S, Feng L, Psimoulis P, Moschas F, Saltogianni V, Jiang Y, Papazachos C, Panagiotopoulos DG, Karagianni E, Vamvakaris D. Recent geodetic unrest at Santorini Caldera, Greece. *Geophys Res Lett* 2012;39(6).
- [26] Nomikou P, Carey S, Papanikolaou D, Croff Bell K, Sakellariou D, Alexandri M, Bejelou K. Submarine Volcanoes of the Kolumbo volcanic zone NE of Santorini Caldera, Greece. *Global Planet Change* 2012;90–91(2012):135–51.
- [27] Nomikou P, Croff Bell K, Carey S, Bejelou K, Parks M, Antoniou V. Submarine volcanic morphology of Santorini Caldera, Greece. Vol. 14, EGU2012-6053, 22–27 April, Vienna: 2012.
- [28] Nomikou P, Papanikolaou D, Alexandri M, Sakellariou D, Rousakis G. Submarine volcanoes along the Aegean volcanic arc. *Tectonophysics* 2013;597–598:123–46.
- [29] Parks MM, Biggs J, England P, Mather TA, Nomikou P, Palamartchouk K, Papanikolaou X, Paradissis D, Parsons B, Pyle DM, Raptakis C, Zacharis V. Evolution of Santorini Volcano dominated by episodic and rapid fluxes of melt from depth. *Nat Geosci* 2012;5(10):749–54.
- [30] Peterson DW, Tilling RI. Transition of basaltic lava from pahoehoe to aa, Kilauea Volcano, Hawaii: field observations and key factors. *J Volcanol Geoth Res* 1980;7(3):271–93.
- [31] Pyle DM, Elliott JR. Quantitative morphology, recent evolution, and future activity of the Kameni Islands volcano, Santorini, Greece. *Geosphere* 2006;2:253–68.
- [32] Riguzzi F, Pietrantonio G, Baiocchi V, Mazzoni A. Water level and volume estimations of the Albano and Nemi lakes (central Italy). *Ann Geophys* 2008;51(4):563–73.
- [33] Rivera J, Lastras G, Canals M, Acosta J, Arrese B, Hermida N, Micallef A, Tello O, Amblas D. Construction of an oceanic island: Insights from the El Hierro (Canary Islands) 2011–2012 submarine volcanic eruption. *Geology* 2013;41(3):355–8.
- [34] Robson GR. Thickness of Etnean lavas. *Nature* 1967;216:251–2.
- [35] Roth RB, Thompson J. Practical application of multiple pulse in air (MPIA) Lidar in large-area surveys. In: *Proceedings of international archives of the photogrammetry, remote sensing and spatial information sciences*, 37 (Part 1), 2008. p. 183–8.
- [36] Sigurdsson H, Carey S, Alexandri M, Vougioukalakis G, Croff KL, Roman C, Sakellariou D, Anagnostou C, Rousakis G, Ioakim C, Gogou A, Ballas D, Misaridis T, Nomikou P. Marine investigations of Greece's Santorini volcanic field. *EOS* 2006;87(34):337–42.
- [37] Smellie JL, Wilch TJ, Rocchi S. 'A'a lava-fed deltas: a new reference tool in paleoenvironmental studies. *Geology* 2013;41(4):403–6.
- [38] Sparks RSJ, Pinkerton H, Hulme G. Classification and formation of lava levees on Mount Etna, Sicily. *Geology* 1976;4(5):269–71.
- [39] Stevenson JA, Mitchell NC, Mochrie F, Cassidy M, Pinkerton H. Lava penetrating water: the different behaviours of pahoehoe and 'a'a at the Nesjahraun, Þingvellir, Iceland. *Bull Volcanol* 2012;74(1):33–46.
- [40] Toth CK. Calibrating Airborne LIDAR Systems. In: *Proceedings of ISPRS Commission II Symposium, Xi'an, China, August 20–23, 2002*. p. 475–80.
- [41] Wadge G, Lopes RMC. The lobes of lava flows on Earth and Olympus Mons, Mars. *Bull Volcanol* 1991;54(1):10–24.
- [42] West S. From volcano to green mountain: a note on Cyrene's beginnings. *Palamedes* 2012;7:43–66.